CHAPTER II

LOW-DIMENSIONAL SEMICONDUCTOR NANOSTRUCTURES: QUANTUM CONFINEMENT AND ITS EFFECT ON OPTICAL PROPERTIES

2.1 Basic Concepts of Low-Dimensional Nanostructures

The content of this chapter deals with the dimensional confinement that affects the electronic and optical properties of semiconductor materials. One of the most noticeable characteristics of these semiconductor structures is delocalization of electrons that can spread their wavefunctions over a larger distance [31]. Over the past two decades, rapid progress in semiconductor fabrication technology, especially in the fabrication of nanostructures, has allowed semiconductor materials to be constructed with a confined electron structure. By reducing the size or dimension of a material into a micrometer and then to a nanometer scale of the order of the de Broglie wavelength of an electron, dramatic changes in electronic and optical properties were observed in these structures [32]. First, if one dimension is reduced into a nano-scale while the other dimensions remain large, then this structure is called a ***quantum well*** [33]. After that two dimensions are reduced while the other remains large, this structure is called a ***quantum wire*** [34]. The extreme case of this process is in which the size is reduced in all three dimensions into a nano-range, as a result, this structure is called a ***quantum dot*** [35], and a donut-shaped quantum dot is called a ***quantum ring*** [36]. All these structures are associated with the name ***quantum*** because changes in electrical and optical properties of these structures after reducing their sizes arise from the quantum mechanical nature of physics as the consequences of the ultra small size. The electronic structures of bulk materials and atom-like nanostructures are different [37-38]. The electronic structures in the case of atom-like nanostructures are characterized by *discrete energy level*s while those of bulk crystal structures are characterized by *bands*. The density of states of bulk semiconductors and low-dimensional nanostructures may be calculated by using quantum mechanics. In that case the band offset between the low-dimensional nanostructures and the surrounding materials provide the energy potential to confine carriers [39-41].

To calculate the electronic states of bulk materials and nanostructures, the effective-mass approximation can effectively be used. The main assumption of the effective-mass approximation is that the envelope wavefunction does not significantly

vary in the unit cell with a length scale of the nanostructure. This assumption can be applied to all low-dimensional nanostructures. Assuming the parabolic band dispersion, band-edge electron states of a semiconductor can then be described by the Schrödinger equation.

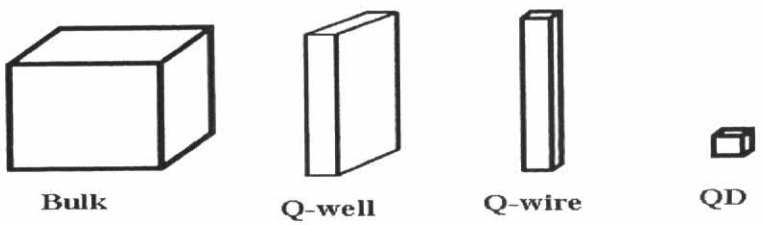

Figure 2.1 Progressive generation of rectangular nanostructures (After Ref. [37]).

Figure 2.2 Progressive generation of curvilinear nanostructures (After Ref. [37]).

Table 2.1 Quantum-confined behavior of semiconductor nanostructures.

Quantum structure	**Delocalization dimensions**	**Confinement dimensions**
Bulk	3(x,y,z)	0
Quantum well	2(x,y)	1(z)
Quantum wire	1(z)	2(x,y)
Quantum dot	0	3(x,y,z)

2.1 Bulk Material

In bulk, the conduction electrons are delocalized in a volume and their wavefunctions spread in three dimensions. By considering the electrons in bulk as free electron gas, the electrons are free to wander around the crystal without being influenced by the potential of the atomic nuclei. A free electron has a velocity v and a momentum $p = mv$. Its energy consists entirely of kinetic energy, and the potential energy tends to be zero ($V = 0$). Therefore, the total energy (E) of the bulk material can be considered as

$$E_{bulk} = E(k) = \frac{\hbar^2 k^2}{2m^*} \tag{2.1}$$

$$D_{bulk} = \frac{1}{2\pi^2}\left(\frac{2m^*}{\hbar^2}\right)^{\frac{3}{2}} E^{\frac{1}{2}} \tag{2.2}$$

where D is the density of states and k is electron wave number, $k = (k_x, k_y, k_z)$.

2.1.2 Quantum Wells

Quantum wells are a type of structure in which a thin layer of smaller-bandgap semiconductor is sandwiched between two layers of wider-bandgap semiconductors. The heterojunction between the smaller- and the wider-bandgap semiconductors forms a potential well confining the electrons and holes within the smaller-bandgap material region. So the electrons are quantized in the direction of confinement, say the z direction, and this becomes the model of particles in a one-dimensional box. The electronic energy levels in the other two dimensions are not discrete and are given by the effective-mass approximation as

$$E_{n,k_x,k_y} = E(c) + \frac{n^2\hbar^2}{8m_e^* l_z^2} + \frac{\hbar^2(k_x^2 + k_y^2)}{2m_e^*} \tag{2.3}$$

where $n = 1, 2, 3,$ are the quantum numbers, the first term $E(c)$ in the right-hand side is the energy corresponding to the bottom of the conduction band, the second term corresponding to the quantized energy, and the third term gives the kinetic

energy of the electron in the x-y plane in which electrons are free to move. The density of states for a quantum-well structure is given by

$$D_{Qwells}(E) = \frac{m}{\pi\hbar^2}\sum_i H(E - E_i) \tag{2.4}$$

where i = 1, 2, 3, . and H (E-E_i) is the ***Heaviside's unit step*** function. It takes the value 0 when E is less than E_i, and 1 when E is equal to or greater than E_i. E_i is the i^{th} eigen-energy level within the quantum well.

2.1.3 Quantum Wires

Quantum wires represent two-dimensional confinements of electrons and holes. Such confinement permits free-electron behavior in only one direction, along the length of the wire, says, the z direction. For this reason, the system of quantum wires may be described as one-dimensional electron gas, where electrons are present in the conduction band. A quantum wire can be cylindrical with a circular cross section as well as rectangular or square in the lateral x-y plane. A representative model of quantum wire in this thesis is a rectangular one with lateral dimensions l_x and l_y. The electronic energy levels of a quantum wire are given by

$$E_{n,k_x,k_y} = E(c) + \frac{n^2\hbar^2}{8m_e^* l_x^2} + \frac{n^2\hbar^2}{8m_e^* l_y^2} + \frac{\hbar^2 k_z^2}{2m_e^*} \tag{2.5}$$

The energy of the one-dimensional quantum wire consists of a sum of four parts. The first term is due to the continuous band value given by the effective-mass approximation. The second and the third terms mention the quantization of electrons in the confinement directions, and the fourth term gives the kinetic energy of the electron in the z direction where electron is free to move. For this case, the density of states is given by

$$D_{Qwires}(E) = \frac{1}{\pi}\left(\frac{2m}{\hbar^2}\right)^{\frac{1}{2}}\sum_i H\frac{n_i(E - E_i)}{(E - E_i)^{\frac{1}{2}}} \tag{2.6}$$

where once again, $H(E-E_i)$ is the Heaviside's unit step function, and n_i is the degeneracy factor. For quantum structures with dimensions lower than 2, it is possible for the same energy levels to occur for more than one arrangement of confined states. To account for this, a second factor $n_i(E)$ has been introduced.

2.1.4 Quantum Dots

A quantum dot represents the three-dimensional confinement of carriers; electrons and holes are confined in the three-dimensional quantum box, whose typical dimensions range from nanometers to tens of nanometers. The detail of the quantum dot will be discussed in next section. The electronic energy levels of the quantum dot are given by

$$E_n = \frac{\hbar^2}{8m_e^*}\left(\frac{n_x^2}{l_x^2}+\frac{n_y^2}{l_y^2}+\frac{n_z^2}{l_z^2}\right) \tag{2.7}$$

The density of states for the zero-dimensional quantum dot is

$$D_{Qdots}(E) = \sum_{E_n} \delta(E-E_n) \tag{2.8}$$

where δ (E-E_i) is the delta function (sharp peak) and $D(E)$ always has discrete values. A discrete value of $D(E)$ produces a sharp peak in the absorption and the emission spectrum of quantum dots even at room temperature. This kind of behavior is for the ideal case, however, due to other side effects, broadening of spectrum is generally observed in reality.

2.1.5 Quantum Rings

A quantum ring represents a donut-shaped quantum dot. It is similar to a quantum wire bent into a loop. A noticeable property of the quantum ring is that the magnetic field effect in a quantum ring can give a novel result for future nano-devices which are based on the magnetic field. The nature of the electronic state is strongly affected by the magnetic flux and its properties are changed when the magnetic flux is penetrating into it. The energy distributions of electrons in bulk, quantum-well,

quantum-wire and quantum-dot structures under a low carrier-density limit condition, where electrons obey the *Boltzmann's distribution statistics*, are illustrated in Fig. 2.3.

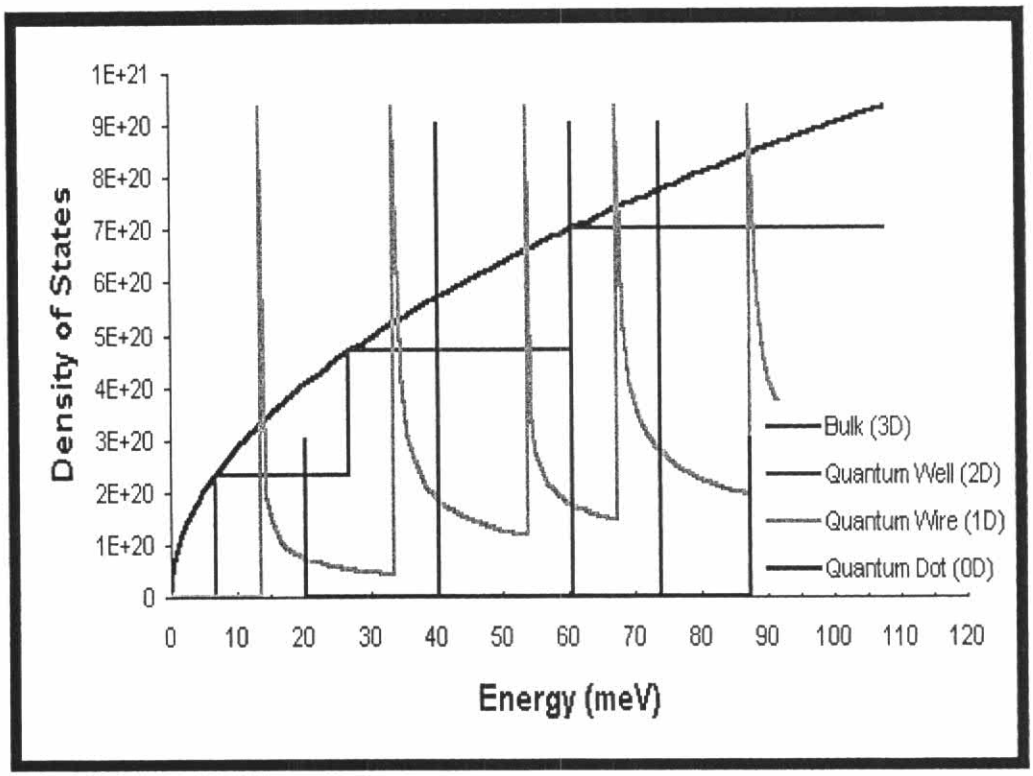

Figure 2.3 Nature of electron density of states in bulk, quantum well, quantum wire, and quantum dot.

2.2 Effect of Quantum Confinement on Optics of Semiconductor Nanostructures

Quantum confinement produces a number of important effects in the electronic and optical properties of semiconductor nanostructures. This effect is very useful for future electronic and optoelectronic device applications. Since this thesis is based on optical characterizations of low-dimensional quantum dot structures, only the quantum confinement effect which is important in relation with the optical properties [37-38] will be discussed in this section. The optical processes of nanostructures are summarized in the tree diagram below.

Tree diagram: Optics of quantum-confined semiconductors

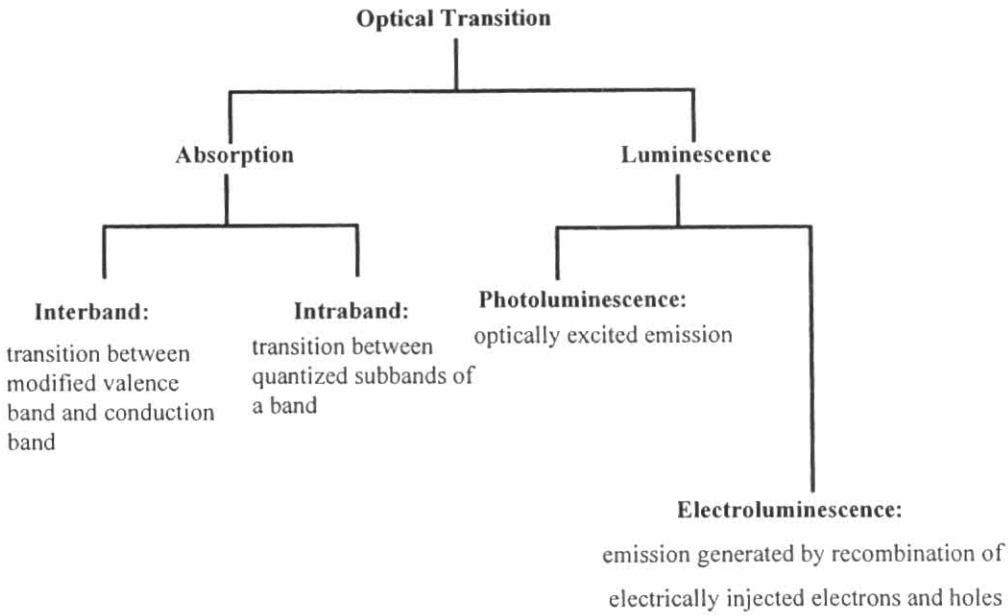

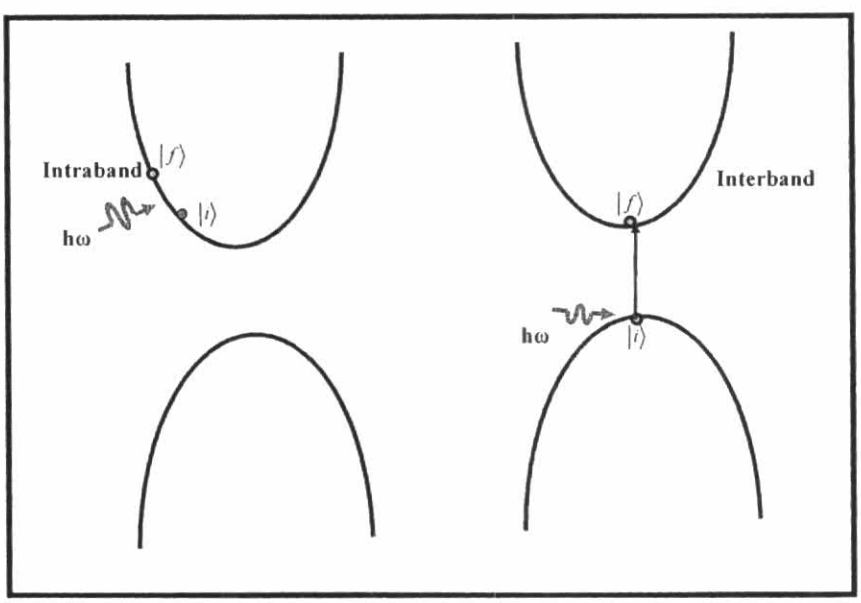

Figure 2.4 Intraband and interband scattering of an electron from an initial state to a finial state.

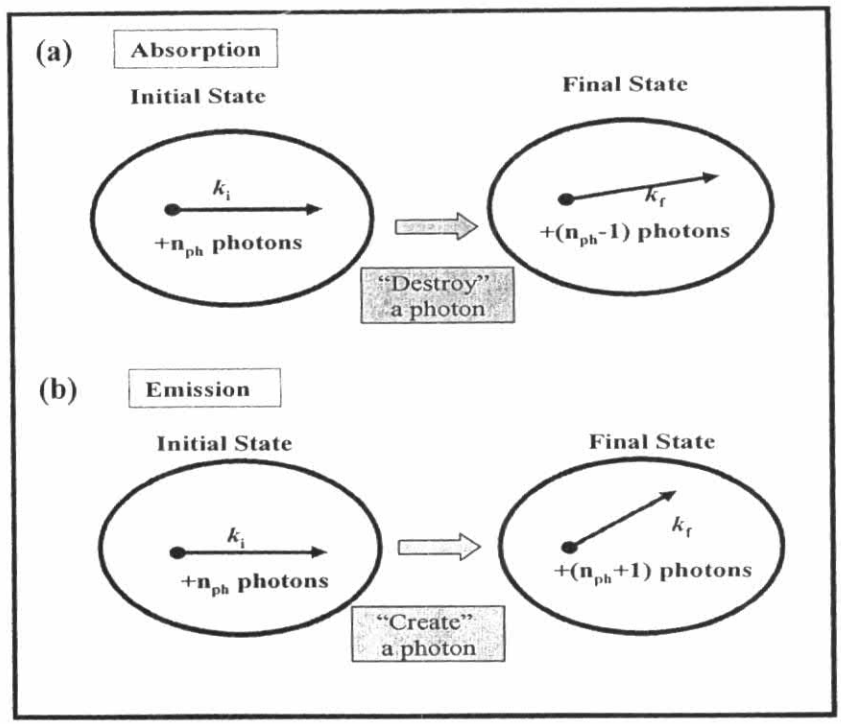

Figure 2.5 (a) Schematic diagram of an absorption process where a photon is absorbed (destroyed) and the energy and the momentum of the electron is altered (upper figure),
(b) The emission of a photon where a photon is created (lower figure).

2.2.1 Size Effect on Optical Properties

Many experimental studies proved that nanostructures of dimensions 1 to 10 nm exhibits fairly narrow optical transitions that are size-dependent. Since the quantum confinement affects the bandgap of the nanostructure, higher quantum confinement gives increasing bandgap as well as appearance of discrete subbands corresponding to quantization along the direction of confinement. Therefore, the structure of a certain size shows optical transition (absorption and emission) at a given frequency. When the size of the structure is increased, the bandgap decreases, and thus the optical resonance shifts to the lower frequency (longer wavelength), and finally approaching the bulk value for a large-enough size.

2.2.2 Increase of Oscillator Strength

As explained in Section 2.1, quantum confinement produces a major modification in the density of states, both for the valence band and the conduction bands. Instead of continuous, smooth distribution of the density of states, the energy is squeezed in a narrow energy range. This packing of energy states near the bandgap becomes more pronounced as the dimensions of confinement increase from bulk, to quantum well, quantum wire, and then quantum dot. For the quantum dots, the density of states has non-zero values only at discrete (quantized) energies. The oscillator strength of an optical transition for an interband transition depends on the joint density of states of energy levels in the conduction band and the valence band, between which the optical transition occurs. Furthermore, it also depends on the overlap of the envelope wavefunctions of electrons and holes. Both these factors produce a large enhancement of oscillator strength upon a quantum confinement. This effect is quite pronounced in quantum wires and quantum dots which are more confined structures (two-dimensionally and three-dimensionally, respectively).

2.2.3 New Intraband Transition

In bulk, the valence band consists of the light-hole band (LH), the heavy-hole band (HB) and the split-off band. The three subbands are separated by the spin-orbit interaction. The absorption of photons with the right energy can result in transition from LH-to-HH, SO-to-HH, or SO-to-LH band, depending on the doping and temperature of the sample or as the result of charge injection introduced by a bias field (e.g. photoinjection). In bulk, transition from one level to another level within the conduction band or the valence band requires a change of quasi-momentum and thus becomes allowed only by the coupling with lattice phonons, which can provide a momentum change. The probability for an intraband transition in bulk semiconductor to occur is low compared with an interband transition in which there is no requirement to change k value.

In quantum-confined nanostructures, there are subbands characterized by the different quantum numbers (n = 1, 2, 3,) corresponding to quantization along the direction of confinement (growth). Thus, for the conduction band, the electron can jump from one sublevel to another without changing its quasi-momentum k. These

new transitions are in IR and have been utilized to produce inter-subband detectors and lasers. These intraband transitions still require the presence of a carrier in the conduction band (electron) or in the valence band (hole). The absorption coefficient for an intraband transition increases rapidly when the size of the nanostructure is decreased. However, for quantum wells, for example, the electronic states are no longer confined within the well, which therefore produces a leveling-off of the absorption coefficient.

2.2.4 Increased Exciton Binding Energy

Quantum confinement of electrons and holes also leads to enhanced binding energy between them and produces increased exciton binding energy compared with the exciton binding energy for bulk materials. For example, a simple theoretical model predicts that the Coulomb interaction between free electrons and holes in a two-dimensional system, or the quantum well, is four times higher than that in bulk. However, actual binding energy is somewhat smaller than in the bulk because the wavefunction of the carriers penetrates into the barrier nearby. This binding produces the excitonic state just below the bandgap, giving rise to the sharp excitonic peaks at temperatures where the exciton binding energy is higher than the thermal energy. Thus, excitonic resonances are very pronounced in quantum-confined structures and, in the strong confinement condition, can be seen even at room temperature.

2.2.5 Dielectric Confinement Effect

Quantum-confined structures also exhibit the dielectric confinement effect produced by the difference in the dielectric constant of the confined semiconductor region and the confining potential around it. However, quantum wells, quantum wires and quantum dots, depending on the method of fabricating and processing, may be embedded in the different semiconductor or a dielectric such as glass or polymer. These quantum structures may be encapsulated by organic ligands, dispersed in a solvent or simply surrounded by air. If the dielectric constant of the surrounding medium is significantly lower than that of the confined semiconductor region, there will be important manifestations derived from different dielectric confinements.

2.2.6 Increase of Transition Probability in Indirect-Bandgap Semiconductors

In the case of an indirect-bandgap semiconductor, the bottom of the conduction band and the top of the valence band do not have the same wave vector k. Thus, emission is not probable in the bulk form, for example, in bulk silicon. However, in a quantum-confined structure, confinement of the electrons produces a reduced uncertainty Δx and increased uncertainty Δk in its quasi-momentum. Confinement, therefore, relaxes the quasi-momentum Δk selection rule, and thus allowing the enhanced emission to be observed in porous silicon and silicon nano-particles.

2.2.7 Nonlinear Optical Properties Caused by the Quantum Confinement Effect

Quantum-confined materials also exhibit enhanced nonlinear optical effects, compared to the corresponding bulk materials. A primary effect is the intensity-dependent changes in optical absorption, derived from a number of processes such as phase-space filling and bandgap renormalization. These processes are manifested at high excitation intensities.

A new optical transition is manifested on binding of excitons to produce bi-excitons. Pronounced changes in optical spectra are observed by applying an electric field along the confinement direction. This is called the *quantum-confined Stark effect* and can be utilized in electro-optic modulator.

2.3 Quantum Dots and Physics Behind Them

Three-dimensional quantum-confined structures, that is, quantum dots (QDs), are solid-state systems that may consist of many atoms. Nevertheless, many experiments have shown in many ways that they behave like a simple quantum system. Here, only conduction-band electrons and valence-band holes are considered, and imagine that everything else can be incorporated into the effective potential acting on these particles, their effective masses, and the dielectric constant of the crystal. The goal here is to describe aspects of the behaviour of idealized quantum dots that are relevant to this thesis.

2.3.1 Energy Levels

Many theoretical calculations have been attempted to explain the energy levels of quantum dots. Among these, the most complicated numerical model is the model that includes realistic shapes and the effects of strain [42-44]. The parameters of the assumed structures strongly affect the result of the energy levels of the quantum dots. But, to gain a qualitative understanding, energy levels are often calculated by using the effective-mass approximation [45], which assumes a single electron in the conduction band of a periodic semiconductor and ignoring its spin. For a plane wave with momentum k, its wavefunction can be written as

$$\psi_e(r) = e^{ik.r} u_{e,k}(r) \tag{2.9}$$

where $u_{e,k}(r)$ is periodic: $u_{e,k}(r+R) = u_{e,k}(r)$, where R is any lattice vector. In the effective-mass approximation, the wavefunction of an electron that experiences a slowly varying potential in a direct-bandgap semiconductor is approximated as

$$\psi_e(r) = f(r) u_{e,0}(r) \tag{2.9-a}$$

where $f(r)$ is the envelope function, which satisfies the Schrödinger equation:

$$\left[-\frac{\hbar^2}{2m^*} \nabla^2 + V(r) \right] f(r) = Ef(r) \tag{2.10}$$

where m^* is the effective mass, related to the curvature of the conduction band at $k = 0$, $V(r)$ is effective potential coming from different band offsets of different materials, and E is the energy of the state. In buried QDs (quantum-confined tiny region which is surrounded by another semiconductor material), the confining barrier V is of finite height as defined by the band offset of two different materials.

Let us assume that self assembled quantum dots are highly flattened in the growth direction (in z direction) comparing with lateral dimensions (x and y direction). It has been reported that the energy level spacing in the z direction can be fairly constant [46]. Thus commonly chosen potential for this kind of structure is

$$V(r) = \begin{cases} \frac{1}{2} m^* \omega_0^2 (x^2 + y^2) & \text{for } |z| < \frac{L}{2} \end{cases} \quad (2.10\text{-a})$$

$$V(r) = +\infty \text{ for } |z| > \frac{L}{2} \quad (2.10\text{-b})$$

where L defines the height of the quantum dots. The energy levels resulting from this Hamiltonian are [47]

$$E = (n_x + n_y + 1)\hbar\omega_0 + (\frac{\pi^2 \hbar^2}{2m^* L^2}) n_z^2 \quad (2.10\text{-c})$$

where n_x and n_y are integers ≥ 0, and n_z is an integer ≥ 1. Usually, L is assumed to be small, so that only the $n_z = 1$ states are considered. For InAs quantum dots, the spacing $\hbar\omega_0$ between the lowest two electron energy levels is typically in the range of 30-80 meV. The relevant wavefunctions that satisfy Eq. 2.10 are:

$$f(R) = H_{n_x}(x) H_{n_y}(y) e^{-\frac{1}{2}\frac{m^* \omega_0}{\hbar}(x^2 + y^2)} \cos(\frac{\pi z}{l}) \quad (2.10\text{-d})$$

where H_n are the Hermite polynomials [47]. A schematic diagram of the energy levels is shown in Fig. 2.6.

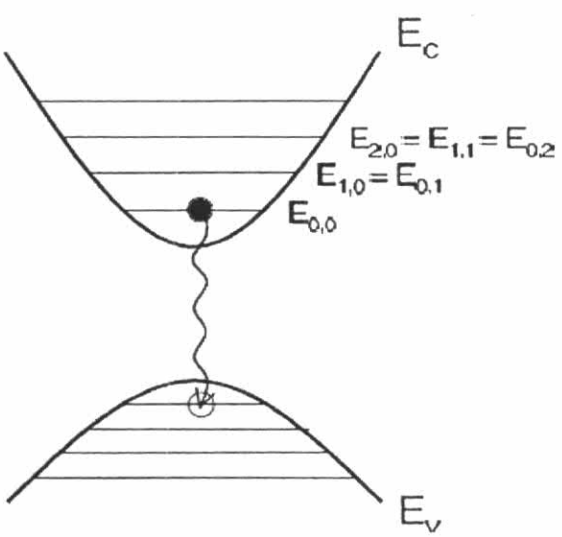

Figure 2.6 Energy band diagram of quantum dot: A radiative transition from the lowest energy level in the conduction band to the highest energy level in the valence band is indicated.

For electrons in the conduction band, the atomic orbital functions contained in $u_{e,0}(r)$ have s-like symmetry, and there is a spin degeneracy in the conduction band. There is complicated situation for the holes in the valence band, because the corresponding atomic orbital functions have p-like symmetry in the valence band. There are three bands (heavy-hole, light-hole, split-off) which can "mix" in the conduction band [45].

When studying quantum dots, only the heavy holes in the valence band have been taken into account in calculation, for simplicity. It is assumed that the highest valence-band state (the hole "ground state") has a heavy-hole nature when the quantization axis is taken to be z, the axis of symmetry. It is often further assumed that the splitting between the first heavy-hole state and the first light-hole state is large, so that the light-hole states can be neglected in the perturbation-theory calculations. The periodic component of the heavy-hole states can be written as $\left|m_j = 3/2\right\rangle = \left|m = 1, \uparrow\right\rangle, \left|m_j = -3/2\right\rangle = \left|m = 1, \downarrow\right\rangle$, where m and m_j are the z projections of the orbital angular momentum and the total angular momentum, respectively.

2.3.2 Spontaneous Emission

The spontaneous emission of electron-hole pairs inside quantum dots is described in this section. Scull *et al* [48] explained the quantum-optic portion of the quantum dot by the following equation, which uses the Hamiltonian describing a quantum dot interacting with modes of the electromagnetic field in the dipole approximation.

$$H = \sum_i E_i \left|i\right\rangle\left\langle i\right| + \sum_{k,\varepsilon} \hbar\omega_k a^{\dagger}_{k,\varepsilon} a_{k,\varepsilon} + \hbar \sum_{k,\varepsilon} \sum_{i,j} g_{ij,k\varepsilon} [a^{\dagger}_{k,\varepsilon} + a_{k,\varepsilon}] \left|j\right\rangle\left\langle i\right| \qquad (2.11)$$

where $\left|i\right\rangle, \left|j\right\rangle$ are quantum-dot levels with energies $E_{i,}$ E_j and $a_{k,\varepsilon}$ are the photon annihilation operators for wavevector k and polarization ε. The coupling coefficient $g_{ij,k\varepsilon}$ between the atom and field modes are given by the equation [48]

$$g_{ij,k\varepsilon} = \left(\frac{\omega_k}{2\varepsilon_0 \hbar V}\right)^{\frac{1}{2}} \varepsilon . \mu_{ij} \qquad (2.12)$$

where $\mu_{ij} = e\langle i|r|j\rangle$ is the atomic transition dipole moments, and V is the volume of the box chosen in quantizing the electromagnetic field. The spontaneous emission from the lowest-energy electron-hole state will be discussed in this section. When electron-hole pairs are injected into a quantum dot slowly (weak excitation), electrons and holes from the higher excited state rapidly relax to the lowest state via intraband transition with the help of phonon emission, after which, the conduction-band electrons return back to the valence band by the radiative recombination. The transition is primarily radiative and the luminescence due to such transition may be seen. The lifetime of the transition is normally in the order of 1 ns. Emission from higher excited states becomes prominent while the strong excitation is used. In such a case, the carriers are injected into the quantum dots quickly and the ground-state recombination is too fast to keep pace with the carrier injection, and thus, the quantum dots begin to be filled with carriers.

The lowest-energy state which consists of one electron-hole pair is supposed to be called "one-exciton" state and there are four terms in this one-exciton state, represented by $\{|\sigma, m_j|\}$ in which σ is the electron spin which value is $\sigma = \pm\frac{1}{2}$ and m_j is the total angular momentum (assuming heavy holes) which value is $m_j = \pm\frac{1}{2}$, both projected along the z axis Firstly, a *very small* quantum dot is considered to calculate the dipole moment for the transition, in which a non-interacting-particle approximation is used [48].

$$\mu_{ab} = e\delta_{\sigma,-\frac{m_j}{3}} \int \psi_e^*(r)\, r\, \psi_h(r) d^3r \tag{2.13}$$

where, ψ_e (r) and, ψ_h (r) are the total wavefunction of electron and hole. The δ function appears because the spin of the electron is conserved in a dipole transition. Next the valence band counterpart is inserted into above equation and the equation expands over lattice sites.

$$\mu_{ab} = \delta_{\sigma,-\frac{m_j}{3}} \int d^3r f^*(r) g(r) \frac{1}{\Omega} \int_{\Omega} u_{e,0}^*(r') er u_{h,m,0}(r') d^3r' \tag{2.14}$$

$$\mu_{ab} = \delta_{\sigma,-\frac{m_j}{3}} \int f^*(r) g(r) \mu_{cv} \frac{x + imy}{\sqrt{2}} d^3r' \tag{2.15}$$

where Ω is the volume of one unit cell, $m = \pm 1$ is the atomic orbital angular momentum of the hole (the same sign as m_j), and $f(r)$ and $g(r)$ are the electron and hole envelope function in the effective-mass approximation, respectively. In the second equation, the integral is replaced by a μ_{cv}, which is a standard material parameter, multiplied by a unit vector corresponding to the orbital angular momentum of the hole. The first term in the above equation is the spin conservation term. It indicates the existence of the bright and dark excitons. For dark excitons, the spins do not match and an open transition cannot occur until the spin of either electron or hole gets flipped. For bright excitons, the spin of the electron match with the spin of the hole. The last term gives the vector dimension of the dipole moment, leading to the polarization selection rule. The angular momentum of the atomic orbital wavefunction of the hole is transferred to the total angular of the emitted photon. The transition strength depends on the overlap between the electron and hole wavefunction. The Hamiltonian in the above equation can be satisfied by using the following equation.

$$H = \hbar\omega_{ab}|a\rangle\langle a| + \sum_{k,\varepsilon}\hbar\omega_k a^{\dagger}_{k,\varepsilon}a_{k,\varepsilon} + \hbar\sum_{k,\varepsilon}(g^{*}_{k,\varepsilon}|a\rangle\langle b|a_{k,\varepsilon} + g_{k,\varepsilon}a^{\dagger}_{k,\varepsilon}|b\rangle\langle a|) \quad (2.16)$$

where $\hbar\omega_{ab}$ is the energy difference between the state $|a\rangle$ and $|b\rangle$, and $g_{k,\varepsilon} = g_{ba,k\varepsilon}$. In the initial state at time t = 0, the system consisting a bright exciton and zero photons is $|a\rangle|0\rangle$, where $|0\rangle$ denotes the vacuum state of the electromagnetic field. At finite time, this state evolves into,

$$|\psi(t)\rangle = c_a(t)e^{-i\omega_{ab}t}|a\rangle|0\rangle + \sum_{k,\varepsilon}c_{b,k,\varepsilon}(t)e^{-i\omega_k t}|b\rangle a^{\dagger}_{k,\varepsilon}|0\rangle \quad (2.17)$$

in which ω_k is the frequency of mode k, Schrödinger's equation with the Hamiltonian in Eq. 2.16 provides differential equations relating the complex functions $c_a(t)$ and $c_{b,k,\varepsilon}(t)$ which determine the time evolution of the state. These equations can be solved in the Weisskopf-Wigner approximation, which assumes that ω_k varies only

little over the linewidth of the transition, which is true in our case ($\frac{\delta\omega}{\omega_{ab}} \approx 10^{-6}$). The result of this calculation is:

$$c_a(t>0) = e^{-(\Gamma/2)t} \tag{2.18}$$

and

$$c_{b,k,\varepsilon}(t>0) = g_{k,\varepsilon}\frac{1-e^{-i(\omega_{ab}-\omega_k)t-\Gamma t/2}}{i(\omega_{ab}-\omega_k)t+\Gamma t/2} \tag{2.19}$$

$$\Gamma = \frac{n\omega_{ab}^3 |\mu_{ab}|^2}{3\pi\varepsilon_0\hbar c^3} \tag{2.20}$$

The final state of the emitted photon is

$$|\gamma\rangle = \sum_{k,\varepsilon} g_{k,\varepsilon}\frac{e^{-i\omega_k t}}{(\omega_k - \omega_{ab}) + i\frac{\Gamma}{2}}a_{k,\varepsilon}^{\dagger}|0\rangle \tag{2.21}$$

The spatial form of the photon wave packet is obtained by taking the Fourier transform of the above result, using $a_{k,\varepsilon}^{\dagger} \propto \sum_r \exp(ik.r)a_{r,\varepsilon}^{\dagger}$. In the far field ($|k||r| >> 1$), the result for the dipole with angular momentum projection m is

$$|\gamma\rangle = \sum_r \frac{\phi(ct-r)}{|r|}e^{(i\omega_{ab}-\frac{\Gamma}{2})(t-|r|/c)}(\hat{r}\times X_{lm}).a_r^{\dagger}|0\rangle \tag{2.22}$$

where φ is the unit step function and X_{lm} are the vector spherical harmonics. The angular dependence of this function is the same as for the electric field from a classical radiating dipole. The time dependence is a one-sided decaying exponential. The photon is in a pure quantum state.

The spontaneous emission rate Γ depends on the dipole moment μ_{ab}, which depends on the material parameter μ_{cv} and on the overlap between the electron and

hole envelope functions. The parameter $\frac{\mu_{cv}}{e}$ is approximately 1 nm, and can be estimated using $\frac{u_{cv}}{e} = \sqrt{\hbar^2 E_p / 2m_0 E_g^2}$, where E_g is the bandgap and $E_p \approx 24$ eV is a parameter in the Kane model. Therefore when $1/\Gamma > 0.28$ ns, the spontaneous emission rates typically 0.5 ns or longer was observed.

For a larger quantum dot, the electron and the hole become correlated, due to the electrostatic interaction between them. The two particle envelope function $h(r,s)$ is needed to be use in calculation. In this situation, the overlap integral is replaced by $\int d^3 r h(r,r)$. For large quantum dots, where the natural exciton Bohr radius a_B^* is smaller than the quantum-dot radius a, the electron-hole overlap term can become larger than one, scaling as (a/a_B^*) 3/2. The spontaneous emission rate is thus enhanced for larger quantum dots.

Eventually, when the dot size becomes comparable to the wavelength of light in the crystal, the lifetime does not decrease further, but rather the emission becomes directional. The center-of-mass angular momentum of the exciton is transferred into the momentum of the emitted photon, as in quantum-well structures.

2.3.2 Polarization Property

By utilizing the electron and the hole wavefunctions obtained as outlined above, the polarization property for each transition can be theoretically calculated. The polarization property is determined with the localization of the wavefunctions of carriers. In bulk, the electrons and holes can move around in every direction without any restriction; the wavefunctions for them distribute uniformly, and thus the dipole moment which is determined by the overlap integral of the wavefunctions of electrons and holes has no directional dependence. Thus, the emission PL spectrum has no polarization property. When the movement of electrons and holes is restricted with the introduction of the quantum-confined structures, the wavefunctions tend to localize. Especially, the quantum-dot structure produces the complete localization of wavefunctions, which leads to the polarization of the luminescence for each transition [49].